AIChE WILEY InterScience DISCOVER SOMETHING GREAT

ENVIRONMENTAL AND ENERGY ENGINEERING

CFD and Experimental Study on Methane Hydrate Dissociation. Part II. General Cases

Wu-Yang Sean
Dept. of Environmental and Ocean Engineering, University of Tokyo, Tokyo 113-8656, Japan

Toru Sato
Dept. of Environment Systems, University of Tokyo, Kashiwa 277-8563, Japan

Akihiro Yamasaki and Fumio Kiyono
Environmental Fluid Engineering Research Group, National Institute of Advanced Industrial Science and Technology (AIST), Tsukuba 305-8569, Japan

DOI 10.1002/aic.11217
Published online June 8, 2007 in Wiley InterScience (www.interscience.wiley.com).

Rate equations proposed in Part I were extended to dissociation processes induced by different methods such as depressurization, raised temperature, or simultaneous changes in temperature and pressure. For all cases, the dissociation rate of hydrate into the two-phase coexisting region (V-L_W) can be expressed by a general form of the product of the rate constant and the logarithm of the solubility ratio of methane in the aqueous solution, x_R to x_S: x_R is the solubility of methane in the aqueous solution that is hypothetically in equilibrium with the hydrate phase under the dissociation pressure and temperature, and x_S is the equilibrium solubility of methane in water under the same dissociation condition. The virtual solubility of methane, x_R, can be estimated by extrapolating the solubility curve of methane under the conditions in equilibrium with the stable hydrate to the region at which the dissociation occurs by a simple thermodynamic treatment. The dissociation equation was applied to experimental results of dissociation processes induced by depressurization with methane bubble formation. The experimentally observed dissociation rates were well correlated by the rate equation with the dissociation constants determined in Part I. The results suggest that the dissociation equation can be applied generally to dissociation processes that occur by different methods, and the rate constant is a universal parameter within the experimental range examined in this work. © 2007 American Institute of Chemical Engineers *AIChE J,* 53: 2148–2160, 2007
Keywords: methane hydrate, dissociation rate constant, hydrate dissociation model, solubility, depressurization

Introduction

In Part I of this study,[1] the dissociation process of methane hydrate induced by ambient water flow at pressures higher than that of the three-phase (H-L_W-V) boundary line was investigated. The phenomenological equation describing the dissociation rate was derived based on the molar Gibbs free energy difference as the driving force for the dissociation, and the dissociation rate constant was determined from experimental results of the overall dissociation rates and numerical simulation results of the methane concentration profile. Hydrate dissociation could be induced by various methods, such as depressurization, temperature increase, and

Current address of W.-Y. Sean: Asia-Pacific Business Division, International Business Center, Industrial Technology Research Institute, TTD Bldg. 3F, 1-2-18, Mita, Minato-ku, Tokyo 108-0073, Japan.
Correspondence concerning this article should be addressed to A. Yamasaki at aki-yamasaki@aist.go.jp.

inhibitor addition.[2] Hydrate becomes thermodynamically unstable during dissociation. It can be anticipated that the phenomenological dissociation rate equation can be generally applied to the dissociation processes induced by other methods when the molar Gibbs free energy changes contingent on the dissociation processes are incorporated as the driving force. In addition, the dissociation rate constant, the constant of proportionality between the dissociation rate and the driving force, could be generally applied to the dissociation process by different methods. Then, the dissociation constant can be confirmed to be "intrinsic," in the same meaning as described by Bishnoi's group.[3–8]

In Part II of this study, dissociation rate equations for various methods, such as depressurization, temperature increase, and simultaneous changes in temperature and pressure, will be derived on the basis of the Gibbs free energy difference between the unstable hydrate phase and the final stable phases of aqueous solution and vapor as the driving force for the dissociation. The Gibbs free energy changes in the rate equation are expressed in terms of the chemical potentials of methane, of which the terms can be converted to the solubility terms of methane in the aqueous solutions, which can be handled more easily. The dissociation equation was then applied to the process of dissociation by depressurization. Experimental studies on the dissociation of a methane hydrate ball under water flow by depressurization were conducted under various conditions. The experimentally observed dissociation rates were then compared with the values predicted by the dissociation rate equation with the dissociation rate constant, k_{bl}, which was determined in Part I of this study, to examine the applicability of the present treatment.

Simple Thermodynamic Treatment of the Dissociation Process Induced by Depressurization or Temperature Change

Dissociation of hydrate by depressurization

Consider a pressure (P)–mole fraction of methane (x) diagram for the methane–water system as shown in Figure 1. Suppose a stable hydrate phase of which the pressure, P_1, is higher than that for the three-phase (H-L_W-V) coexisting pressure, P_T, for a given temperature, T_1. The thermodynamic state of the hydrate is denoted by point N in Figure 1. When the pressure is dropped abruptly to P_2 ($<P_T$) from P_1, while keeping the temperature constant, the state of the hydrate would be moved from point N to point Q, located in the two-phase (V-L_W) coexisting region. The hydrate phase under such conditions becomes thermodynamically unstable. The hydrate will dissociate into two phases of vapor (denoted by point S) and aqueous solution (denoted by point U), which will finally reach in thermodynamic equilibrium under the dissociation pressure, P_2. During the hydrate dissociation process, three phases of unstable hydrate, vapor, and the aqueous solution would coexist for a given pressure and temperature, but they are not in thermodynamic equilibrium. It might be quite difficult to follow the detail path of the irreversible dissociation processes. In this study, we took a simple and convenient approach to formulate the dissociation rate. We paid attention only to the initial state (unstable hydrate, denoted by Q in Figure 1) and final state (vapor–liquid mixture, denoted by the points S and U, in Figure 1, which is stable under the dissociation condition), and it is assumed that the dissociation rate is in proportional to the difference in the molar Gibbs free energy between the initial state and the final state. Thus, the following linear relationship is assumed between the molar Gibbs free energy difference and the dissociation rate, F_P, namely,

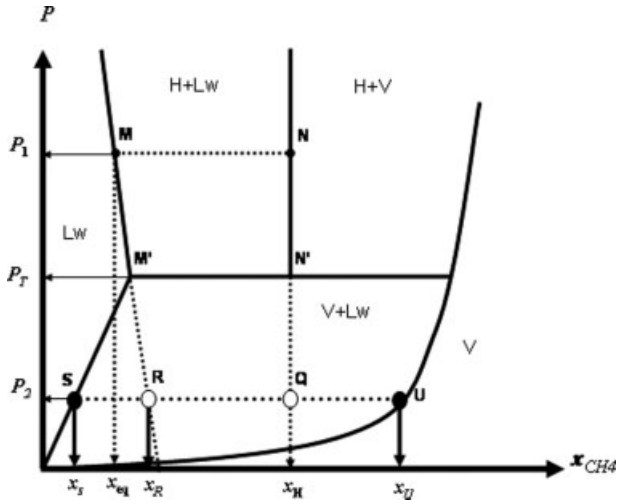

Figure 1. Mole fraction-pressure (*x-P*) phase diagram for methane-water-hydrate (temperature constant).

$$F_P = k_P \Delta G_P, \tag{1}$$

where ΔG_P is the free energy difference as the driving force, k_P is the rate constant for dissociation induced by the pressure reduction.

Driving Force for the Dissociation. The next step is the formulation of the driving force for the dissociation in the terms of free energy. For this purpose, we assumed that the unstable hydrate phase will dissociate at an isobaric and isothermal condition of the dissociation pressure, P_2 and the temperature, T_1. The state of the dissociating hydrate phase can be denoted by the condition at point Q in Figure 1. The isobaric condition may be rationalized by the rapid transfer of the pressure change in the hydrate phase. And the isothermal condition can be rationalized when the ambient water flow rate is high enough to supply the heat of dissociation. When 1 mole of the unstable hydrate phase is converted into the stable two-phases of vapor and liquid, the change of the Gibbs free energy, ΔG_P, may be given by,

$$\Delta G_P = G^H(Q) - \{G^L(S) + G^V(U)\}, \tag{2}$$

where $G^H(Q)$ is the Gibbs free energy of 1 mole of the hydrate at the dissociation pressure, P_2, of which the state is denoted by point Q in Figure 1. $G^V(U)$ and $G^L(S)$ are the Gibbs free energies of the vapor (point U), and the aqueous solution (point S), respectively, to which 1 mole of the hydrate will be converted and partitioned by the dissociation.

Note these two phases of the vapor and the aqueous solution are stable and in equilibrium under the dissociation condition at pressure, P_2, and temperature, T_1.

Since 1 mole of hydrate is consisting of 1 mole of methane and h_w moles of water, where h_w is the hydration number, the molar Gibbs free energy of the hydrate phase, $G^H(Q)$, under the dissociation pressure, P_2, is given by,

$$G^H(Q) = \mu_M^H(Q) + h_w \mu_W^H(Q), \tag{3}$$

where $\mu_M^H(Q)$, and $\mu_W^H(Q)$ are chemical potentials of methane and water in the hydrate phase, respectively, under the dissociation condition of P_2, T_1, of which the state is denoted by point Q in Figure 1.

When 1 mole of the hydrate will be dissociated into 1 mole of methane and h_w moles of water, each component will be partitioned to the vapor (denoted by point U) and the aqueous solution (denoted by point S). Because of the liquid–vapor equilibrium,

$$\mu_M^V(U) = \mu_M^L(S) \ : \text{ for methane}, \tag{4}$$

$$\mu_W^V(U) = \mu_W^L(S) \ : \text{ for water}, \tag{5}$$

where $\mu_M^L(S)$, and $\mu_W^L(S)$ are the chemical potentials of methane and water, respectively, in the aqueous solution at pressure P_2, denoted by point S, and $\mu_M^V(U)$, and $\mu_W^V(U)$ are the chemical potentials of methane and water, respectively, in the vapor phase at pressure P_2, denoted by point U. Because of the phase equilibrium condition in Eq. 4, the sum of the Gibbs free energies of methane in the vapor and that in the aqueous solution is simply given by multiplying the total mole number of methane (= 1 mole) and the chemical potential of methane in either phase, namely, $1 \times \mu_M^V(U) = 1 \times \mu_M^L(S)$. Similarly, that of water is given by, $h_W \times \mu_W^V(U) = h_W \times \mu_W^L(S)$. Thus, the total Gibbs free energy of the two phases of the vapor and the aqueous solution is given by,

$$G^L(S) + G^V(U) = \mu_M^L(S) + h_W \mu_W^L(S) = \mu_M^V(U) + h_W \mu_W^V(U). \tag{6}$$

Therefore, the driving force for the dissociation or the Gibbs free energy difference between the hydrate phase and the sum of the vapor and the aqueous solution is given by,

$$\begin{aligned} \Delta G_P &= G^H(Q) - \{G^L(S) + G^V(U)\} \\ &= \{\mu_M^H(Q) - \mu_M^L(S)\} + h_w\{\mu_W^H(Q) - \mu_W^L(S)\} \\ &= \{\mu_M^H(Q) - \mu_M^V(U)\} + h_w\{\mu_W^H(Q) - \mu_W^V(U)\}. \end{aligned} \tag{7}$$

Formulation of the Free Energy Difference in Terms of the Solubilities. The Gibbs free energy terms in Eq. 7 can be converted into to the terms of the solubility of methane in aqueous phase by simple thermodynamic assumptions.

Hydrate Phase. When the hydrate phase is in equilibrium with other stable phase such as vapor or liquid, the chemical potentials of water and methane in the hydrate phase are equal to those in the phase in equilibrium. When the hydrate phase is in equilibrium with the aqueous solution phase, the chemical potentials could be expressed in terms of the equilibrium solubility of methane in water. Such expressions of chemical potentials cannot be used for the hydrate under the dissociation because no stable aqueous phase exists in equilibrium with the unstable hydrate. In this study, a hypothetical aqueous solution phase was considered for the expression of chemical potential of the unstable hydrate phase. The hypothetical aqueous solution is assumed to be (hypothetically) in equilibrium with the hydrate under the dissociation pressure. Then, the chemical potentials in the hydrate phase under the dissociation pressure were expressed in terms of the solubility in the hypothetical aqueous solution phase. The state of the hypothetical aqueous solution is denoted by point R in Figure 1, which is located on the extrapolated equilibrium solubility curve, MM′, to the dissociation pressure, P_2 from the three-phase coexisting pressure, P_T. The solubility terms can be calculated by extrapolation under the assumption that the equilibrium relationship between the hydrate phase and the aqueous solution phase above the three-phase coexisting pressure, P_T, is hold to the dissociation pressure, P_2. The extrapolation method of the solubility in the hypothetical aqueous solution will be discussed in the following section. It should be noted that the hypothetical aqueous solution does not exit or emerge during the dissociation process.

Because of the low solubility of methane in the aqueous solution, the hypothetical aqueous solution could be assumed to be an ideally dilute solution with water as the solvent, and methane as the solute. Thus, the activity coefficients can be set at unity for both components, the chemical potentials of methane and water in the (unstable) hydrate phase can be expressed by,

For methane:

$$\mu_M^H(Q) = \mu_M^L(R) = \mu_M^* + RT_1 \ln x_R, \tag{8}$$

For water:

$$\mu_W^H(Q) = \mu_W^L(R) = \mu_W^0 + RT_1 \ln(1 - x_R), \tag{9}$$

where μ_M^* and μ_W^0 are the chemical potentials of the reference states, and x_R is the equilibrium solubility of methane in the hypothetical aqueous solution (denoted by R) in equilibrium with the hydrate phase at the dissociation pressure, P_2. The reference state for water is the chemical potential of pure water ($x_R = 0$). The reference state for methane is set as $x_R \to 0$, where the activity coefficient is unity.[9]

Aqueous Solution Phase. Stable aqueous solution under the dissociation condition is assumed to be an ideally dilute solution with water as the solvent, and methane as the solute and the chemical potentials of the components can be expressed by,

For methane:

$$\mu_M^L(S) = \mu_M^V(U) = \mu_M^* + RT_1 \ln \ x_S, \tag{10}$$

For water:

$$\mu_W^L(S) = \mu_W^V(U) = \mu_W^0 + RT_1 \ln(1 - x_S), \tag{11}$$

where μ_M^* and μ_W^0 are the chemical potentials of the same reference states as those in Eqs. 8 and 9, respectively, and x_S is the solubility of methane in the stable aqueous solution (point S) in equilibrium with the vapor phase at the dissociation pressure, P_2.

Therefore, the free energy difference, ΔG_P, can be given by,

$$\Delta G_P = G^H(Q) - \{G^L(S) + G^V(U)\} = RT_1 \ln\frac{x_R}{x_S} + h_W RT_1 \ln\frac{1-x_R}{1-x_S}. \quad (12)$$

Since the solubilities of methane in water, x_R, x_S, are extremely low (in the order of 10^{-6}–10^{-7}), and the hydration number, h_w, is about 5–6, the second term in the right hand side of Eq. 12 can be neglected in comparison to the first term. Then, the free energy difference, ΔG_P, can be approximated by,

$$\Delta G_P = RT_1 \ln\frac{x_R}{x_S}. \quad (13)$$

Note that Eq. 13 could be directly derived by considering only the chemical potential difference of methane between in the hydrate phase and in the aqueous solution. By inserting Eq. 13 into Eq. 1, the rate equation can be written as,

$$F_P = k_P RT_1 \ln\frac{x_R}{x_S}. \quad (14)$$

Thus, the dissociation equation can be simply expressed by the mole fraction of methane in the hypothetical solution in equilibrium with the hydrate, x_R, at the dissociation pressure, and the equilibrium solubility of methane in the aqueous solution, x_S, which is stable at the dissociation pressure. Note that Eq. 14 is similar to Eq. 12 in the Part I of this study. The ratio of the mole fractions can be replaced by the ratio of the volumetric molar concentrations because of the extremely low mole fractions of methane dissolved in water, namely,

$$F_P = k_P RT_1 \ln\frac{C_R}{C_S}, \quad (15)$$

where C_R and C_S are the volumetric molar concentration of methane [mol/m^3] in the hypothetical aqueous solution equilibrated with the hydrate under the dissociation condition and that in the stable aqueous solution at the same condition, respectively.

Estimation of the Solubility of Methane in the Hypothetical Aqueous Solution, x_R. To estimate the solubility of methane in the hypothetical aqueous solution, x_R, the following thermodynamics was used to extrapolate the solubility curve in the H-L_W region (MM′) to the L_W-V region.

Suppose a stable hydrate (denoted by point N) in equilibrium with an aqueous solution (denoted by point M) at a pressure, P_1, of which the state is located in the H-L_W region. The equilibrium relation of methane between the hydrate phase and the aqueous phase can be written as:

$$\mu_M^H(N) = \mu_M^H(P_1, T_1, x_H) = \mu_M^L(M) = \mu_M^L(P_1, T_1, x_{eq}), \quad (16)$$

where x_H is the molar ratio of the methane in the hydrate phase, and x_{eq} is the solubility of methane in the aqueous solution equilibrated with the hydrate phase. When there is an infinitesimal change in pressure on the equilibrium line under an isothermal condition, Eq. 16 can be written as

$$\mu_M^H(P_1, T_1, x_H) + \left[\frac{\partial \mu_M^H}{\partial P}\right]_{T=T_1} dP = \mu_M^L(P_1, T_1, x_{eq}) + \left[\frac{\partial \mu_M^L}{\partial P}\right]_{T=T_1} dP, \quad (17)$$

On the equilibrium line, Eq. 17 becomes

$$\left[\frac{\partial \mu_M^H}{\partial P}\right]_{T=T_1} = \left[\frac{\partial \mu_M^L}{\partial P}\right]_{T=T_1}. \quad (18)$$

On the other hand, with an assumption of the ideally dilute solution, the chemical potential of methane in the aqueous solution at pressure P and temperature T can be written as

$$\mu_M^L(P, T, x) = \mu_M^*(P, T) + RT \ln x, \quad (19)$$

Differentiating Eq. 18 with a constant temperature leads to

$$\left[\frac{\partial \mu_M^L}{\partial P}\right]_{T=T_1} = \left[\frac{\partial \mu_M^*}{\partial P}\right]_{T=T_1} + RT\left[\frac{\partial \ln x}{\partial P}\right]_{T=T_1}. \quad (20)$$

From the thermodynamics,

$$\left[\frac{\partial \mu_M^*}{\partial P}\right]_{T=T_1} = v_L, \quad (21)$$

where v_L is the molar volume of methane dissolved in water. Neglecting the effect of pressure on the cage occupancy, x_H, in the hydrate phase, we have

$$\left[\frac{\partial \mu_M^H}{\partial P}\right]_{T=T_1} = v_H, \quad (22)$$

where v_H is the molar volume of methane in the hydrate phase. By combining Eqs. 18 and Eqs. 20–22, we obtain:

$$v_H = v_L + RT\left[\frac{\partial \ln x}{\partial P}\right]_{T=T_1}. \quad (23)$$

By integrating Eq. 23 from P_1 to P_2 under an isothermal condition and rearranging, we have:

$$RT_1 \ln\frac{x_R}{x_{eq}} = (v_H - v_L)(P_2 - P_1). \quad (24)$$

Assuming that there is a very small change in the solubility, and thus neglecting terms over the second order, we obtain

$$RT_1 \ln\frac{x_R}{x_{eq}} = RT_1 \ln\left(1 + \frac{x_R - x_{eq}}{x_{eq}}\right) \approx RT_1 \frac{x_R - x_{eq}}{x_{eq}} = (v_H - v_L)(P_2 - P_1). \quad (25)$$

Finally, the aqueous solubility of methane, x_R, can be expressed as a linear equation of pressure, P_1:

$$x_R = x_{eq}\left[\frac{(v_H - v_L)(P_2 - P_1)}{RT_1} + 1\right]. \quad (26)$$

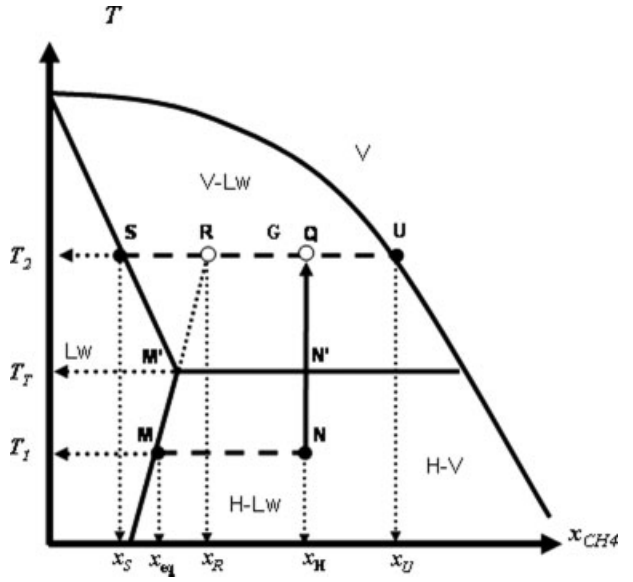

Figure 2. Mole fraction-pressure (*x*-*T*) phase diagram for methane-water-hydrate (pressure constant).

Experimental results have demonstrated an almost linear relationship between the solubility of methane and the pressure in the H-L_W region.[10] Thus, it would be reasonable to extrapolate the solubility curve to the V-L_W region based on Eq. 26.

Dissociation by temperature change

To consider the dissociation process that takes place on changing the temperature, a temperature–mole fraction of methane ($x - T$) phase diagram is useful for the methane–water system as shown in Figure 2. Suppose a stable hydrate of which the thermodynamic state is located in the two-phase (V-L_W) coexisting region denoted by point N in Figure 2. The hydrate is stable because the temperature, T_1, is below the three-phase (H-L_W-V) coexisting temperature, T_T for a given pressure, P_1. When temperature is raised abruptly from T_1 to T_2 ($>T_T$) while keeping the pressure constant ($P = P_1$), the state of the hydrate moved to point Q, which is located in the V-L_W two-phase coexisting region, and the hydrate will become unstable. Hence, the hydrate will be dissociated into two phases of vapor (denoted by point U) and aqueous solution (denoted by point S), which are stable and in equilibrium under the dissociation condition. Note the thermodynamic states of denoted by points, S, U are different from those in the previous section.

A linear phenomenological relationship is assumed between the dissociation rate, F_T and the free energy difference, ΔG_T, between the unstable hydrate phase (denoted by Q) and the stable two-phase of liquid (denoted by S) and vapor (denoted by U). Then the dissociation rate can be expressed by,

$$F_T = k_T \Delta G_T, \tag{27}$$

where k_T is the rate constant for the dissociation due to the temperature change.

Driving force for the dissociation: It is assumed that the temperature and the pressure conditions of the hydrate phase are constant during the dissociation process, which is equal to the dissociation pressure, P_1, and temperature T_2. The driving force for the hydrate dissociation is assumed to be the change of the Gibbs free energy when the hydrate at temperature T_2 (denoted by point Q) is dissociated into two phases of vapor (denoted by point U) and aqueous solution (denoted by point S). When 1 mole of the hydrate consisting 1 mole of methane and h_w moles of water (h_w is the hydration number) under the dissociation temperature, T_2, is dissociated into the two phases of vapor and aqueous solution, the Gibbs free energy change, ΔG_T, can be expressed by the following equation,

$$\begin{aligned}\Delta G_T &= G^H(Q) - \{G^L(S) + G^V(U)\} \\ &= \{\mu_M^H(Q) - \mu_M^L(S)\} + h_w\{\mu_W^H(Q) - \mu_W^L(S)\} \\ &= \{\mu_M^H(Q) - \mu_M^V(U)\} + h_w\{\mu_W^H(Q) - \mu_W^V(U)\},\end{aligned} \tag{28}$$

where $\mu_M^H(Q)$ and $\mu_W^H(Q)$ are chemical potentials of methane and of water, respectively, in the hydrate phase under the dissociation condition of P_1, T_2, denoted by point Q; $\mu_M^L(S)$ and $\mu_W^L(S)$ are the chemical potentials of methane and of water, respectively, in the aqueous solution, denoted by point S; $\mu_M^V(U)$ and $\mu_W^V(U)$ are the chemical potentials of methane and water, respectively, in the vapor phase, denoted by point U. Note a similar treatment to that used in the previous section was applied for summing the Gibbs free energies of the two phases of vapor and aqueous solution to derive Eq. 28. Equation 28 is essentially the same form as Eq. 7 in the previous section, except the thermodynamic condition assigned to each term.

Formulation of the Free Energy Difference in Terms of the Solubilities. Similar treatment used in the previous section can be applied for the present system with the assumption of the ideally dilute solutions.

Hydrate Phase. The chemical potential of methane and water in the hydrate phase at the dissociation temperature, T_2 (denoted by point Q in Figure 2), is assumed to be represented by that in the hypothetical aqueous solution (denoted by point R), which is in equilibrium with the hydrate phase at the dissociation temperature, T_2. The equilibrium solubility of methane in the hypothetical aqueous solution, x_R, can be obtained by extrapolating the solubility curve (MM′) from the H-L_W region to the V-L_W region under an isobaric condition. The aqueous solution is assumed to be an ideally dilute solution with water as the solvent, and methane as the solute. The molar Gibbs free energy of the hydrate phase at the dissociation temperature can be expressed by,

$$\begin{aligned}G^H(Q) = G^L(R) = (\mu_M^* + RT_2 \ln x_R) \\ + h_w\{\mu_W^0 + RT_2 \ln(1 - x_R)\},\end{aligned} \tag{29}$$

where μ_M^* and μ_M^0 are the chemical potentials of the reference states, which are same as in Eqs. 8 and 9, respectively.

The Aqueous Phase. The aqueous solution is approximated with an ideally dilute solution with water as the solvent, and methane as the solute, and the total Gibbs free energy of the two phases can be expressed by,

$$G^{L}(S) + G^{V}(U) = (\mu_M^* + RT_2 \ln x_S) + h_w\{\mu_W^0 + RT_2 \ln(1 - x_S)\}, \quad (30)$$

where μ_M^* and μ_M^0 are the chemical potentials of the same reference states same as them in Eqs. 8 and 9, respectively, and x_S is the equilibrium solubility of methane in water at the dissociation temperature, T_2. Therefore, the free energy difference, ΔG_T, can be given by,

$$\begin{aligned}\Delta G_T &= G^{H}(Q) - \{G^{L}(S) + G^{V}(U)\} \\ &= G^{L}(R) - \{G^{L}(S) + G^{V}(U)\} \\ &= RT_2 \ln\frac{x_R}{x_S} + h_w RT_2 \ln\frac{1 - x_R}{1 - x_S}. \end{aligned} \quad (31)$$

Since the solubilities of methane in water, x_R, x_S are extremely low (in the order of $10^{-6} - 10^{-7}$), and the hydration number, h_w, is about 5–6, the second term in the right hand side of Eq. 31 can be neglected in comparison to the first term. Then the free energy difference, ΔG_T, can be approximated by,

$$\Delta G_T = RT_2 \ln\frac{x_R}{x_S}. \quad (32)$$

Equation 32 is essentially the same as Eq. 13. By inserting Eq. 32 into Eq. 28, the rate equation can be rewritten as,

$$F_T = k_T RT_2 \ln\frac{x_R}{x_S}. \quad (33)$$

The ratio of the mole fractions is equivalent to the ratio of the volumetric molar concentrations because of the extremely low mole fractions of methane dissolved in water, namely,

$$F_T = k_T RT_2 \ln\frac{C_R}{C_S}, \quad (34)$$

where C_R and C_S are the volumetric molar concentrations of methane [mol/m^3] in the hypothetical aqueous solution equilibrated with the hydrate at the dissociation temperature, T_2, and that in the aqueous solution that is stable at the same temperature, respectively.

Extrapolation of the Solubility Curve. The aqueous solubility curve of methane in the H-L_W region can be extrapolated to the L_W-V region by the thermodynamic method similar to that used in the previous section. In the H-L_W region, the equilibrium relation for methane between the hydrate phase and the aqueous phase is given by,

$$\mu_M^H(N) = \mu_M^H(P_1, T_1, x_H) = \mu_M^L(M) = \mu_M^L(P_1, T_1, x_{eq}). \quad (35)$$

When there is an infinitesimal change in temperature with keeping the pressure on the equilibrium line, Eq. 35 can be written as

$$\mu_M^H(P_1, T_1, x_H) + \left[\frac{\partial \mu_M^H}{\partial T}\right]_{P=P_1} dT = \mu_M^L(P_1, T_1, x_{eq}) + \left[\frac{\partial \mu_M^L}{\partial T}\right]_{P=P_1} dT. \quad (36)$$

On the equilibrium line, Eq. 36 becomes

$$\left[\frac{\partial \mu_M^H}{\partial T}\right]_{P=P_1} = \left[\frac{\partial \mu_M^L}{\partial T}\right]_{P=P_1}. \quad (37)$$

On the other hand, the chemical potential of methane in the water phase at temperature T is given by assuming an ideally dilute solution,

$$\mu_M^L(P, T, x) = \mu_M^*(P, T) + RT \ln x. \quad (38)$$

Differentiating Eq. 38 with respect to T, we obtain

$$\left[\frac{\partial \mu_M^L}{\partial T}\right]_{P=P_1} = \left[\frac{\partial \mu_M^*}{\partial T}\right]_{P=P_1} + \left[\frac{\partial (RT \ln x)}{\partial T}\right]_{P=P_1}. \quad (39)$$

Neglecting the effect of temperature on the cage occupancy in the hydrate phase, we have

$$\left[\frac{\partial \mu_M^H}{\partial T}\right]_{P=P_1} = -s_H, \quad (40)$$

where s_H is the molar entropy of methane in the hydrate. From thermodynamics,

$$\left[\frac{\partial \mu_M^*}{\partial T}\right]_{P=P_1} = -s_L, \quad (41)$$

where s_L is the molar entropy of methane in the aqueous phase.

Equations 37 and 39–41 can be combined to give

$$s_H = s_L - \left[\frac{\partial (RT \ln x)}{\partial T}\right]_{P=P_1}. \quad (42)$$

Integrating Eq. 42 from (T_1, x_{eq}) to (T_2, x_R) with respect to T gives,

$$RT_2 \ln x_R - RT_1 \ln x_{eq} = -(s_H - s_L)(T_2 - T_1); \quad P = P_1. \quad (43)$$

Equation 43 can be rearranged to

$$\ln x_R = \frac{1}{T_2}\frac{T_1}{R}\{R \ln x_{eq} + (s_H - s_L)\} - \frac{1}{R}(s_H - s_L); \quad P = P_1. \quad (44)$$

Finally, the solubility, x, can be expressed as an exponential function of temperature T_2:

$$x_R = x_0 \exp\left(\frac{a}{T_2}\right), \quad (45)$$

where x_0 and a are constants that are given by,

$$x_0 = \exp\left\{-\frac{1}{R}(s_H - s_L)\right\}, \quad (46)$$

$$a = \frac{T_1}{R}\{R \ln x_{eq} + (s_H - s_L)\}, \quad (47)$$

In this case, a linear extrapolation of the solubility curve to the H-V region is not appropriate. Nonlinear curve fitting

by two parameters based on Eq. 45 could be conducted based on the real solubility curve in the H-L_W region.

Dissociation by simultaneous changes in temperature and pressure

In practical cases for the production of methane from the methane hydrate layer, both depressurization and heating would be used simultaneously to increase the production rate. In this section, the dissociation process induced by simultaneous changes in the temperature and the pressure will be discussed. For such cases, a three-dimensional *P-T-x* phase diagram (not shown) should be used.

Suppose a stable hydrate (denoted by point *N*) at temperature, T_1, and pressure, P_1. When temperature and pressure are changed to T_2 and P_2, respectively, which is located in the two-phase (V-L_W) region, the hydrate phase (denoted by point *Q*) will become unstable and be dissociated into two phases of vapor (denoted by point *U*) and aqueous solution (denoted by point *S*), which are stable and in equilibrium under the dissociation condition. Again, the thermodynamic states associated with points *S*, *U* are different from the ones in the previous sections. The dissociation rate can be expressed by,

$$F_S = k_S \Delta G_S = k_S [G^H(Q) - \{G^L(S) + G^V(U)\}], \tag{48}$$

where k_S is the rate constant for the dissociation due to simultaneous changes in pressure reduction and temperature. $G^H(Q)$ is the molar Gibbs free energy of the hydrate, consisting 1 mole methane and h_w moles of water under the dissociation condition. $G^V(U)$ and G^L(S) are the Gibbs free energies in the aqueous phase and the vapor phase, respectively, into which 1 mole of the hydrate will be dissociated and partitioned. The terms of the Gibbs free energy in Eq. 48 can be reduced to the chemical potential terms by a similar procedure to that used in the previous section.

$$\begin{aligned}\Delta G_S &= G^H(Q) - \{G^L(S) + G^V(U)\} \\ &= \{\mu_M^H(Q) - \mu_M^L(S)\} + h_w\{\mu_W^H(Q) - \mu_W^L(S)\} \\ &= \{\mu_M^H(Q) - \mu_M^V(U)\} + h_w\{\mu_W^H(Q) - \mu_W^V(U)\},\end{aligned} \tag{49}$$

which is essentially same as Eqs. 7 and 28. With the assumption that the aqueous solutions are ideally dilute solutions, the Gibbs free energy difference can be expressed by,

$$\begin{aligned}\Delta G_S &= G^H(Q) - \{G^L(S) + G^V(U)\} \\ &= G^L(R) - \{G^L(S) + G^V(U)\} \\ &= RT_2 \ln\frac{x_R}{x_S} + h_w RT_2 \ln\frac{1 - x_R}{1 - x_S},\end{aligned} \tag{50}$$

where x_R is the solubility of methane in the hypothetical aqueous solution, which is in equilibrium with the hydrate phase under the dissoication condition. x_S is the equilibrium solubility of methane in water under the same dissociation condition. Equation 50 is similar to Eqs. 12 and 31 in the previous sections. Again, the terms for the water can be neglected and finally, the driving force can be written,

$$\Delta G_S = RT_2 \ln\frac{x_R}{x_S}, \tag{51}$$

and the dissociation rate can be expressed by the volume concentration terms,

$$F_S = k_S RT_2 \ln\frac{C_R}{C_S}. \tag{52}$$

In the same manner as for the previous cases, the aqueous solubility curve of methane in the H-L_W region can be extended to the L_W-V region and expressed as a function of pressure and temperature:

$$x = x'_0 \exp\left(\frac{a'P}{T}\right), \tag{53}$$

where a' and x'_0 are constants. In this case, the dependencies of the solubility curve on the temperature and the pressure are necessary to determine the hypothetical solubility curve based on Eq. 53.

The dissociation rate for each dissociation method can be expressed by product of the dissociation constant with the logarithm of the ratio of the solubility methane in a hypothetical aqueous solution that is in equilibrium with the hydrate phase under the dissociation condition and the equilibrium solubility of methane under the same dissociation condition. The different dissociation constants were incorporated in the different dissociation methods, such as k_{bl} (concentration change), k_P (pressure change), k_T (temperature change), k_S (simultaneous change in temperature and pressure). These rate constants, however, should be independent of the dissociation methods for a given temperature and pressure condition because all the rate equations were derived based on the same principle that the Gibbs free energy difference between the unstable hydrate phase and the stable phases of vapor and aqueous solution is assumed to be the driving force for the dissociation. In the following section, experimentally-observed dissociation rates of methane hydrate by depressurization will be compared with the rates predicted by Eq. 14 with the dissociation rate constant, k_{bl}, which was determined in Part I of this study. In other words, the applicability of the present treatment as well as the universality of the dissociation rate constant will be checked.

Experimental

Experimental apparatus

The same experimental system as in Part I of this study was used for the depressurization experiments, with a modification by installing an instrument for bubble size measurement, as shown in Figure 3. The observed dissociation rates by depressurization were much faster than those obtained in Part I, and bubble formation near the hydrate ball was observed because of the higher dissociation rate. The overall dissociation rate is the sum of the dissolved methane in the water flow and the gasified methane. The overall dissociation rate was measured by measuring the flow rate of methane bubbles after the dissolved methane was gasified by reducing the pressure of the water flow to atmospheric pressure. Since the solubility of methane at atmospheric pressure is negligibly small, the dissociation rate can be determined by the bubble flow rate with a sufficient accuracy. The measurement of the flow rate of the methane bubbles in water was carried

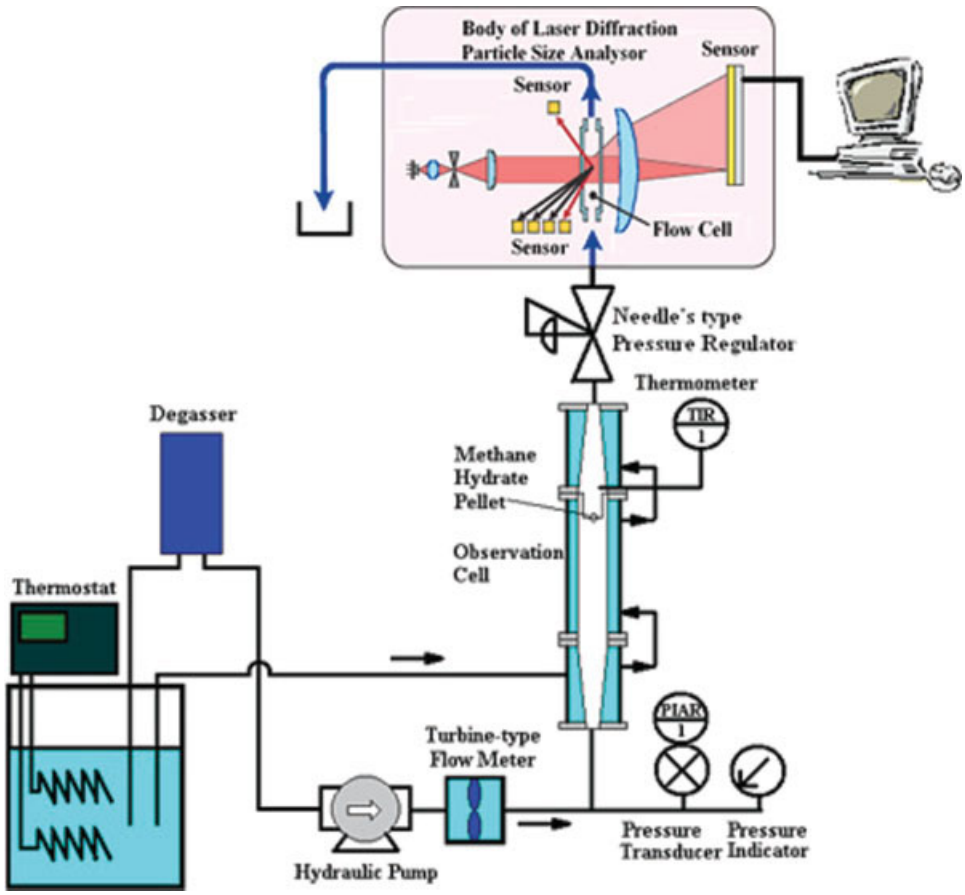

Figure 3. Experimental apparatus for the measurement of the dissociation rate of methane hydrate with bubble formation.

[Color figure can be viewed in the online issue, which is available at www.interscience.wiley.com.]

out using an instrument for particle size distribution measurement by laser scattering (Shimadzu SALD-3100) installed downstream of the pressure-regulating valve (Figure 3). To remove the dissolved gas in the feed water to the dissociation cell, a degassing unit (Yokohama Rika ERC-3000W) was installed before the hydraulic pump.

Experimental procedure

The methane hydrate ball was prepared by the same method described in Part I. The ball was mounted in the flow cell by holding it in a plastic net without wire, to prevent the hydrate ball from detaching from the cell because of the higher dissociation rate. After mounting the hydrate ball, the water flow was started at a pressure and temperature condition, at which the hydrate was thermodynamically stable. Then, the system pressure was changed by adjusting the pressure-regulating valve installed downstream of the observation cell. The water flow was depressurized to the atmospheric pressure after passing through the pressure-regulating valve, and introduced to the instrument for bubble size measurement. The detailed procedure for the bubble size measurement is described in the next section. The flow rate was fixed at 1.78×10^{-5} m^3 s^{-1} for all runs, the temperature was changed in the range of 276.15–282.15 K and the dissociation pressure was set to values from 0.3 to 0.9 MPa below the equilibrium pressure.

Determination of the volumetric flow rate of methane bubbles

When a laser beam is diffracted by a flow of bubbles, the diffraction pattern is given by,

$$I(\theta) = I_0 V \sum_{i=1}^{n} \gamma_i(r_i) I_i'(\theta, r_i), \tag{54}$$

where $I(\theta)$ is the diffraction intensity at the angle, θ; V is the total volumetric flow rate of the bubbles; $\gamma_i(r_i)$ is the volume-based fractional size distribution of the bubbles with radius r_i; $I_i'(\theta, r_i)$ is the nondimensional diffraction intensity per unit volume of bubbles with radius, r_i. $I_i'(\theta, r_i)$ is given by Eq. 55 under the conditions when diffusion and absorption of the laser beam are ignored, and the bubble size is larger than the wavelength of the beam[11]

$$I_i'(\theta, r_i) = \frac{\xi^2}{16\pi^2 r_i^2} \beta_i(r_i)^4 \left[\frac{2J_1(\beta_i(r_i)\sin\theta)}{\beta_i(r_i)\sin\theta}\right]^2, \tag{55}$$

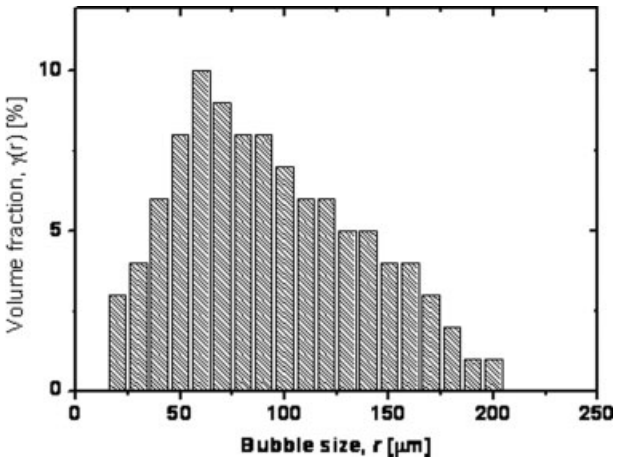

Figure 4. A typical bubble size distribution of the methane bubbles measured by the laser diffraction method.

where $\beta_i(r_i)$ is a parameter defined by $2\pi r_i/\xi$, where ξ is the laser wavelength, and J_1 is the first Bessel function. The parameter, I_0, is an instrumental system-specific constant and independent of the diffraction angle and the bubble radius.

The fractional size distribution of the bubbles, $\gamma_i(r_i)$, can be determined from the experimentally observed diffraction intensity pattern, $I(\theta)$, by using the normalization condition of $\sum\gamma_i(r_i) = 1$, without knowing the values of I_0V in Eq. 54. Figure 4 shows a typical distribution of the bubble size of methane dispersed in water, $\gamma_i(r_i)$, which was determined from the measured diffraction pattern, $I(\theta)$. The product IV_0 can be obtained as the proportionality constant in Eq. 54 with the known size distribution of the bubbles and the measured intensity, $I(\theta)$. To determine the volumetric flow rate of the bubbles, V, equivalent to the dissociation rate of methane hydrate, the system-specific parameter, I_0, should be determined separately. To obtain the value of I_0 for the present system, diffraction pattern was measured with the same apparatus, but using glass beads with a uniform size at 60 μm dispersed in the water flow. The diffraction patterns were measured for various volumetric flow rates of the glass beads, V. In this case, Eq. 54 can be reduced to,

$$I(\theta) = I_0 V I'_{60}(\theta), \tag{56}$$

Since the parameter, $I'_{60}(\theta)$, is constant for beads with a fixed size at 60 μm, and it can be calculated based on Eq. 55, the unknown parameter, I_0, can be determined as the proportionality constant of $I(\theta)$ against the volumetric flow rate, V. Only the intensity for a certain diffraction angle is necessary to determine the parameter I_0. In this study, the principal intensity, $I_{\max}$, the peak of the obtained diffraction pattern against the diffraction angle, θ, was used. In Figure 5, the principal intensity, $I_{\max}$ was plotted against the volume flow rate of the glass beads, and a linear relationship was observed. Thus, the proportionality constant, I_0, was determined from the slope of the line in Figure 5,

$$I_{\max}(\tilde{\theta}) = I_0 I'_{60}(\tilde{\theta}) V, \tag{57}$$

where $\tilde{\theta}$ is the diffraction angle giving the maximum intensity. With a known value of the apparatus-specific parameter I_0, the volumetric flow rate of the methane bubbles can be determined from the measured diffraction intensity and the size distribution $\gamma_i(r_i)$ by,

$$V = \frac{I(\theta)}{I_0 \sum_{i=1}^{n} \gamma_i(r_i) I'_i(\theta, r_i)}. \tag{58}$$

Error analysis was conducted for the measurement of the bubble flow rate by the laser diffraction method. Uncertainties may mainly be originated in the calibration curve, Eq. 56, for the intensity with the volume flow rate of glass beads with 60 μm diameter. It was assumed that the diameter of the glass beads used for the calibration was uniform at 60 μm. We analyzed the error in the volume flow rate when the size distribution of the glass beads is Gaussian with different variations, σ = 1, 2, 3, and 10 μm. As a result, the error in the volumetric flow rate was estimated in the range of -8% to $+14\%$.

Results and Discussion

Dissociation rate equation for depressurization with bubble formation

The dissociation rate equation by the depressurization is given by Eq. 14, which represents the local dissociation rate where the ambient water is saturated with methane. In the dissociation experiments induced by depressurization, bubble formation was observed in the vicinity of the methane hydrate ball. This result indicates that the methane concentration in the vicinity of the methane hydrate ball is saturated, and that excess methane was gasified due to the higher dissociation rate. Therefore, it can be confirmed that Eq. 14 holds for all locations on the hydrate surface, and the overall dissociation rate, F_{obs}, is simply the product of the local flux, F_{P},

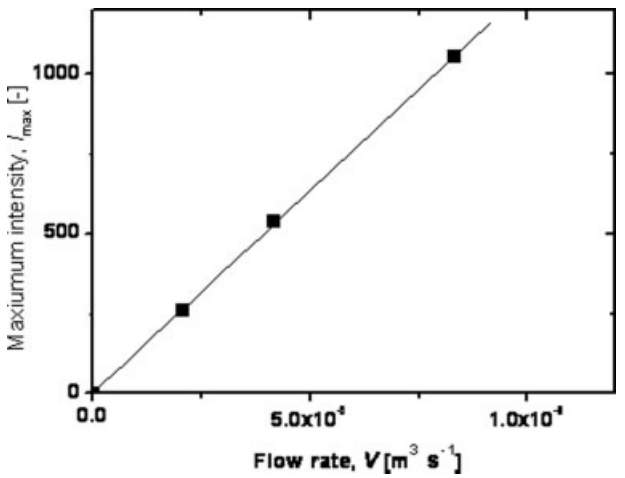

Figure 5. Relationship between the principal laser diffraction intensity, $I_{\max}$, and the volumetric flow rate of glass beads in water, of which the diameter is uniform at 60 μm.

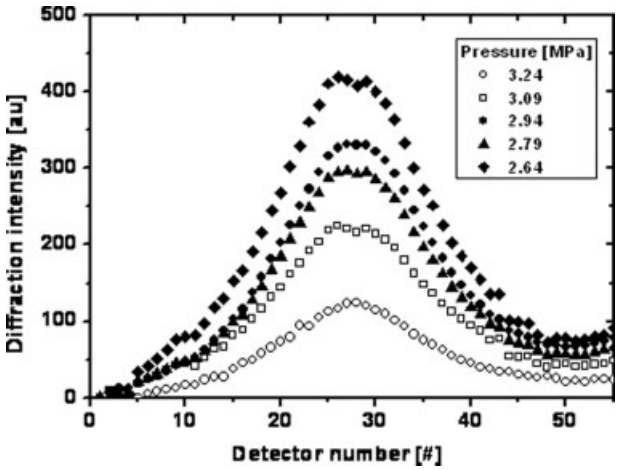

Figure 6. Laser-diffraction intensity with respect to the detectors for various dissociation pressures at T = 276.15 K.

and the surface area. Thus,

$$F_{\text{obs}} = \pi d^2 k_{\text{P}} R T_1 \ln \frac{x_{\text{R}}}{x_{\text{S}}}, \tag{59}$$

where d is the diameter of the methane hydrate ball.

The equilibrium solubility of methane can be correlated by the following empirical equation[12]

$$x_{\text{S}} = \exp[-152.777 + 7478.8 T_1^{-1} + 20.6794 \ln T_1 + 0.753161 \ln(10^{-5} P)]. \tag{60}$$

The same equation as Eq. 28 in Part I can be used for the extrapolation of the solubility curve in the three-phase (H-L_W-V) coexisting region to the two-phase (V-L_W) coexisting region,

$$x_{\text{R}} = 1.0 \times 10^{-3} \times [-0.01P + (2.23 \times 10^{-4}) \times \exp(0.0319 T_1)]. \tag{61}$$

If the rate constant, k_{bl}, obtained in Part I of this study[1] can be applied to the present case (Eq. 62),

$$k_{\text{bl}} = 3.89 \times 10^{12} \exp\left(-\frac{98300}{RT_1}\right), \tag{62}$$

The overall methane hydrate dissociation rate can be expressed by Eq. 63 as a function of temperature only by replacing k_{P} in Eq. 59 with k_{bl} in Eq. 62, then,

$$F_{\text{pred}} = 3.89 \times 10^{12} \times \pi d^2 R T \ln \frac{x_{\text{R}}}{x_{\text{S}}} \exp\left(-\frac{98300}{RT_1}\right) \tag{63}$$

By comparing the experimentally observed dissociation rate, F_{obs}, with the predicted value F_{pred}, with Eq. 63, the applicability of the rate constant, k_{bl}, to the dissociation process induced by depressurization could be examined.

Comparison of the experimental results with the predicted values

A typical measured diffraction intensity for methane bubble flow in water is shown in Figure 6 at T_1 = 276.15 K with respect to the detector number, which is a function of the diffraction angle θ. With a decreasing dissociation pressure, the diffraction intensity increased generally, indicating an increasing dissociation rate, except that the diffraction intensity at the pressure of 2.79 MPa is lower than one at the pressure of 2.94 MPa. This discrepancy may be due to some experimental errors cause by several reasons, e.g., bubbles trapping in the dead volume of the experimental system and the water condensation at the surface of the flow cell (although nitrogen was flown at the surface) due to the low temperature operations. To convert the diffraction intensity to the total bubble volume, V, which is equivalent to the overall dissociation rate of the methane hydrate ball, the determined value of I_0 based on the method described in the previous section was used.

In Figures 7–9, the observed dissociation rates and the predicted values are plotted against the dissociation pressure for temperatures of 276.15, 279.15, and 282.15 K, respectively. The corresponding three-phase coexisting equilibrium pressures were 3.54, 4.82, and 6.56 MPa, respectively. It is also assumed that the temperature during the dissociation is constant at the initial temperature. Note the error bars in the figures denoted the range of the experimental errors for the bubble flow measurements due to the uncertainties in the calibration curve based on the assumption of uniform distribution of particles without overlapping. (Eq. 56). Generally, good agreement was observed between the experimental results and the predicted values for the dissociation rates for all the conditions studied, although the predicted values are slightly higher than the experimental results for a temperature of 276.15 K. The results indicate that the dissociation rate constant, k_{bl}, which was determined as the proportionality rate constant for the dissociation process induced by a fresh water flow, is applicable to the dissociation process induced by depressurization.

Dotted lines in Figures 7–9 denote the values of the dissociation rate predicted by the equation proposed by Kim et al.,[3] in which the fugacity difference between for the

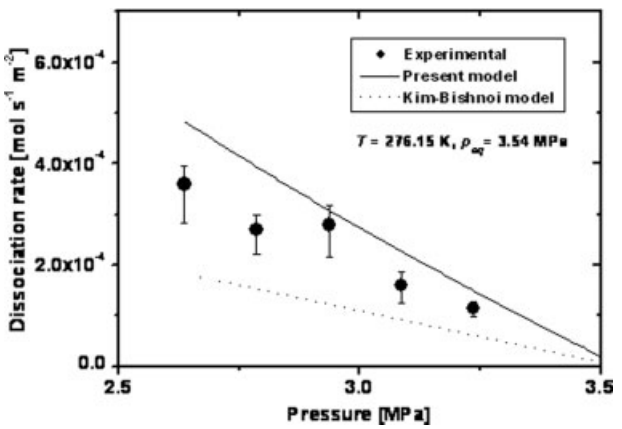

Figure 7. Comparison of the predicted values with the experimental results for the overall dissociation rate of methane hydrate under various pressure conditions.

Water flow rate, $Q = 1.78 \times 10^{-5}$ m^3 s^{-1}, T = 276.15 K.

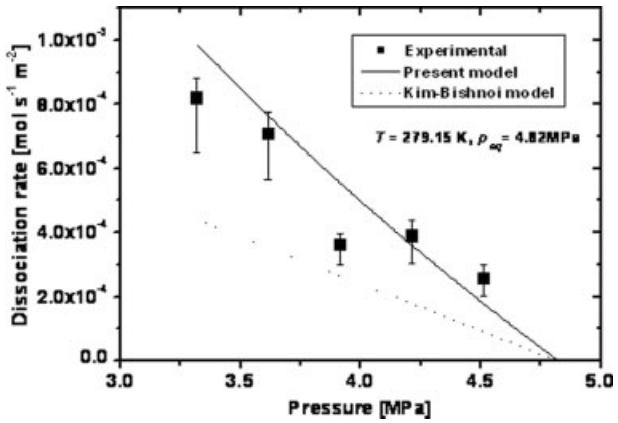

Figure 8. Comparison of the predicted values with the experimental results for the overall dissociation rate of methane hydrate under various pressure conditions.

Water flow rate = 1.78×10^{-5} m^3 s^{-1}, T = 279.15 K.

three-phase (H-L_W-V) coexisting equilibrium condition (pressure, P_T) and for the dissociation condition (pressure, P_2) is the driving force for the dissociation:

$$F_{KB} = k'_{KB} \exp\left(\frac{-\Delta E_{KB}}{RT_1}\right)\{f(P_T, T_1) - f(P_2, T_1)\}, \quad (64)$$

where k'_{KB} is a constant independent of the pressure and temperature, and ΔE_{KB} is the activation energy. The dissociation rate constant in Eq. 64 can be claimed as intrinsic when it was determined from dissociation experiments under such conditions that neither mass nor heat transfer resistance were the rate-determining step. The dissociation rates predicted by the Kim–Bishnoi equation were slightly lower than the experimental results and the values predicted by Eq. 14 developed in this study at lower pressure conditions, but the discrepancy became smaller when the pressure approached the three-phase (H-L_W-V) coexisting equilibrium pressure. The experimental results were in better agreement with the values predicted by Eq. 14 than those predicted by the Kim-Bishnoi equation.

Equation 14 can be reduced to Eq. 64 with the following approximation. The fugacity of the methane, f_M, is given by the following function of the chemical potential,

$$\mu_M^V = \mu_M^{\oplus}(T) + RT \ln f_M(P, T), \quad (65)$$

where $\mu_M^{\oplus}$ is the chemical potential at a standard state where $f_M = 1$. Inserting Eq. 65 into Eq. 14, we obtain

$$F_P = k_P RT_1 \ln \frac{f_M(P_2, T_1)}{f_M(P_1, T_1)}. \quad (66)$$

The fugacity difference of methane between two pressure conditions P_2 and P_1, Δf_M, can be expressed as

$$f_M(P_2, T_1) = f_M(P_1, T_1) + \Delta f_M. \quad (67)$$

Then, Eq. 65 can be expressed as

$$F_P = k_P RT_1 \ln \frac{f_M(P_1, T_1) + \Delta f_M}{f_M(P_1, T_1)}. \quad (68)$$

When the fugacity difference is much smaller than f_M (P_1, T), the logarithm term in Eq. 68 can be approximated by

$$\begin{aligned} F_P &= k_P RT_1 \ln\left[1 + \frac{\Delta f_M}{f_M(P_1, T_1)}\right] \\ &\approx k_P RT_1 \frac{\Delta f_M}{f_M(P_1, T_1)}. \end{aligned} \quad (69)$$

Hence the dissociation equation expressed in terms of the chemical potential difference can be reduced to Eq. 64 expressed by the fugacity difference. The approximation can be rationalized by the experimental results in Figures 7–9, where both equations gave approximately linear dependences of the dissociation rate on the dissociation pressure. In addition, the deviation between the values predicted by Eq. 14 and those predicted by Eq. 64 becomes lower for conditions where the dissoication pressure were close to the three-phase coexisting pressure.

It was shown that the linear phenomenological equation for the hydrate dissociation based on the Gibbs free energy difference can be applied to the dissociation processes driven by pressure changes within the conditions tested in this study. In addition, the rate constant, k_{bl}, determined in Part I of this study, which is obtained from the analysis of the dissociation process induced by a fresh water flow, was found to be applicable to a dissociation process with a different driving force, i.e., depressurization. Although the applicability of the dissociation rate constant as well as the dissociation equation was confirmed within the experimental conditions studied in the present work, it can be anticipated that they could be applied to other dissociation processes with wider ranges of driving forces. For this purpose, additional experimental work should be required to test the present model covering wider ranges of the experimental conditions.

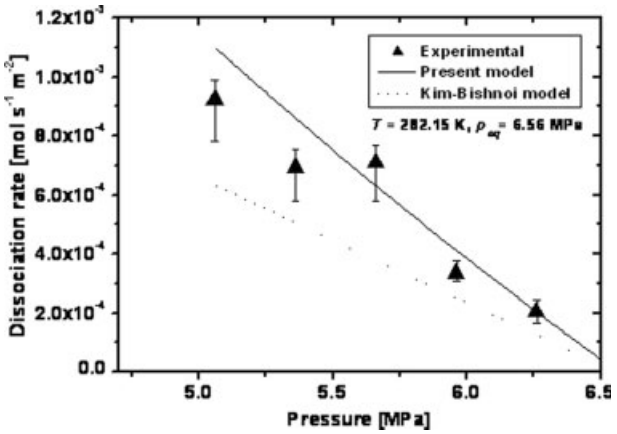

Figure 9. Comparison of the predicted values with the experimental results for the overall dissociation rate of methane hydrate under various pressure conditions.

Water flow rate = 1.78×10^{-5} m^3 s^{-1}, T = 282.15 K.

Conclusions

Rate equations for the dissociation process of methane hydrate, induced by various methods (depressurization, temperature increase, simultaneous change in temperature and pressure), were derived based on the Gibbs free energy difference as the driving force for the dissociation reaction. The driving force for the dissociation can be expressed in a general form with the logarithm of the ratio of the solubilities of methane in water, x_R and x_S, where x_R is the solubility of methane in an hypothetical aqueous solution equilibrated with the hydrate phase under the dissociation condition, and x_S is the equilibrium solubility of methane in water under the dissociation condition. The proportionality constant in the dissociation equation, of which the value was determined in Part I from the dissociation process induced by a fresh water flow, can be applied to predict the dissociation rate of hydrate induced by the depressurization into the two-phase (L_W-V) coexisting region with a sufficient accuracy.

Acknowledgments

This work was financially supported by the MH21 Consortium of Japan. The authors are grateful to Drs. H. Narita and T. Yamaguchi of AIST and Prof. Y. Masuda of University of Tokyo for their helpful comments and encouragement.

Notation

a = parameter defined in Eq. 47, K
a' = parameter defined in Eq. 53, K Pa^{-1}
C = volumetric molar concentration of methane dissolved in water, mol m^{-3}
C_R = volumetric molar solubility of methane in the hypothetical aqueous solution equilibrated with the hydrate phase under the dissociation condition, mol m^{-3}
C_S = volumetric molar solubility of methane in the aqueous solution under the dissociation condition, mol m^{-3}
d = diameter of the methane hydrate ball, m
ΔE = activation energy, J mol^{-1}
ΔE_{KB} = activation energy in Eq. 64, J mol^{-1}
f = fugacity, Pa
F = dissociation flux, mol s^{-1} m^{-2}
F_P = dissociation flux by a pressure change, mol s^{-1} m^{-2}
F_S = dissociation flux by a simultaneous change in pressure and temperature, mol s^{-1} m^{-2}
F_T = dissociation flux by a temperature change, mol s^{-1} m^{-2}
G = Gibbs free energy per one mole of hydrate, J mol^{-1}
ΔG = change of the Gibbs free energy when one mole of the hydrate is dissociated into two phase of the vapor and the aqueous solution, J mol^{-1}
h_w = hydration number
I = diffraction intensity
I_0 = non-dimensional parameter in Eq. 54
I_{60}' = non-dimensional diffraction intensity per unit volume of beads with a uniform radius of 60 μm
I_{max} = principal intensity
I_i' = non-dimensional diffraction intensity per unit volume of bubbles with radius, r_i
J_1 = first Bessel function
k'_{KB} = rate constant for the dissociation in Eq. 64, mol s^{-1} m^{-2} Pa^{-1}
k_{bl} = rate constant for the dissociation by a fresh water flow, mol^2 J^{-1} s^{-1} m^{-2}
k_P = rate constant for the dissociation by a pressure change defined in Eq. 1, mol^2 J^{-1} s^{-1} m^{-2}
k_S = rate constant for the dissociation by a simultaneous change in pressure and temperature, defined in Eq. 48, mol^2 J^{-1} s^{-1} m^{-2}
k_T = rate constant for the dissociation by a temperature change, defined in Eq. 27, mol^2 J^{-1} s^{-1} m^{-2}
P = pressure, Pa
P_T = three-phase (V-H-L_W) coexisting pressure, Pa
R = gas constant, = 8.314 J K^{-1} mol^{-1}
r_i = bubble radius, m
s_H = molar entropy of methane in the hydrate, J K^{-1} mol^{-1}
s_L = molar entropy of methane in the aqueous phase, J K^{-1} mol^{-1}
T = absolute temperature, K
V = total volumetric flow rate of the bubbles, m^3 s^{-1}
v_H = molar volume of methane in the hydrate, m^3 mol^{-1}
v_L = molar volume of methane in the aqueous phase, m^3 mol^{-1}
x = mole fraction of methane
x_0 = parameter defined in Eq. 46
x_0' = parameter defined in Eq. 53
x_{eq} = solubility of methane in the aqueous solution in equilibrium with the stable hydrate phase
x_H = mole fraction of methane in the hydrate
x_R = solubility of methane in the hypothetical aqueous solution in equilibrium with the hydrate phase under the dissociation condition
x_S = solubility of methane in the aqueous solution under the dissociation condition
x_U = mole fraction of methane in the vapor phase under the dissociation condition

Greek letters

β_i = parameter defined by $2\pi r_i/\xi$
γ_i = volume-based fractional size distribution of bubbles with radius r_i
μ = chemical potential, J mol^{-1}
$\mu^{\oplus}$ = chemical potential of methane in the vapor phase at the reference state, J mol^{-1}
μ_M^* = chemical potential of methane at the reference state, J mol^{-1}
μ_M^H = chemical potential of methane in the hydrate phase, J mol^{-1}
μ_M^L = chemical potential of methane in the aqueous solution, J mol^{-1}
μ_M^V = chemical potential of methane in the vapor, J mol^{-1}
μ_W^H = chemical potential of water in the hydrate phase, J mol^{-1}
μ_W^L = chemical potential of water in the aqueous solution, J mol^{-1}
μ_W^V = chemical potential of water in the vapor, J mol^{-1}
μ_W^0 = chemical potential of water at the reference state, J mol^{-1}
θ = diffraction angle, deg
$\tilde{\theta}$ = diffraction angle giving the maximum intensity, deg
σ = deviation of the diameter of the glass beads, m
ξ = laser wavelength, m

Superscripts

H = hydrate phase
L = aqueous solution phase
V = vapor phase

Subscripts

1 = initial state
2 = final state
eq = equilibrium
M = methane
R = hypothetical aqueous solution equilibrated with the hydrate phase under the dissociation condition
S = aqueous solution phase which is stable under the dissociation condition
U = vapor phase which is stable under the dissociation condition
W = water

Literature Cited

1. Sean W-Y, Sato T, Yamasaki A, Kiyono F. CFD and experimental study on methane hydrate dissociation. I. Dissociation under water flow. *AIChE J*. 2007;53:262–274.
2. Sloan ED. *Clathrate Hydrates of Natural Gases*, 2nd ed. New York: Marcel Dekker, 1998.
3. Kim HC, Bishnoi PR, Heidemann RA, Rizvi SSH. Kinetics of methane hydrate decomposition. *Chem Eng Sci*. 1987;42:1645–1653.

4. Jamaluddin AKM, Kalogerakis N, Bishnoi PR. Modeling of decomposition of a synthetic core of methane gas hydrate by coupling intrinsic kinetics with heat-transfer rates. *Can J Chem Eng*. 1989;67:948–954.
5. Dholabhai PD, Kalogerakis N, Bishnoi PR. Kinetics of methane hydrate formation in aqueous-electrolyte solutions. *Can J Chem Eng*. 1993;71:68–74.
6. Bishnoi PR, Natarajan V. Formation and decomposition of gas hydrates. *Fluid Phase Equilib*. 1996;117:168–177.
7. Clarke M, Bishnoi PR. Determination of the intrinsic rate of ethane gas hydrate decomposition. *Chem Eng Sci*. 2000;55:4869–4883.
8. Clarke M, Bishnoi PR. Determination of the activation energy and intrinsic rate constant of methane gas hydrate decomposition. *Can J Chem Eng*. 2001;79:143–147.
9. Wood SE, Battino R. *Thermodynamics of Chemical Systems*. Cambridge: Cambridge University Press, 1990.
10. Seo Y, Lee H, Ryu BJ. Hydration number and two-phase equilibria of CH_4 hydrate in the deep ocean sediments. *Geophys Res Lett*. 2002;29:1244.
11. Society of Powder Technology, Japan. *Handbook of Powder Technology* (in Japanese). Tokyo: Nikkan Kogyo Shimbunsya, 1998.
12. Fogg PGT, Gerrard W. *Solubility of Gases in Liquids*. New York: Wiley, 1991.

Manuscript received Oct. 18, 2006, and revision received Apr. 3, 2007.